AD-A079 927 FOREIGN TECHNOLOGY DIV WRIGHT-PATTERSON AFB OH F/G 20/4
COMPUTATION OF SUPERSONIC SPACE ENCIRCLING FLOW OF BLUNT-NOSED --ETC(U)
JUN 79 Z YOULAN, W RUGUAN, Z XICHANG

UNCLASSIFIED FTD-ID(RS)-T-0645-79 NL

END
DATE FILMED
2-80
DDC

PHOTOGRAPH THIS SHEET

AD A079927

DTIC ACCESSION NUMBER

LEVEL

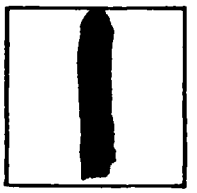

INVENTORY

FTD-ID(RS)T-0645-79

DOCUMENT IDENTIFICATION

DISTRIBUTION STATEMENT A
Approved for public release;
Distribution Unlimited

DISTRIBUTION STATEMENT

ACCESSION FOR	
NTIS	GRA&I
DTIC	TAB
UNANNOUNCED	
JUSTIFICATION	
BY	
DISTRIBUTION /	
AVAILABILITY CODES	
DIST	AVAIL AND/OR SPECIAL
A	

DISTRIBUTION STAMP

DDC
RECEIVED
JAN 28 1980
D

DATE ACCESSIONED

79 11 13 243

DATE RECEIVED IN DTIC

PHOTOGRAPH THIS SHEET AND RETURN TO DTIC-DDA-2

DTIC FORM OCT 79 70A

DOCUMENT PROCESSING SHEET

FTD-ID(RS)T-0645-79

FOREIGN TECHNOLOGY DIVISION

COMPUTATION OF SUPERSONIC SPACE ENCIRCLING FLOW OF BLUNT-NOSED BODY

By

Zhu Youlan, Wang Ruquan, Zhong Xichang

EDITED TRANSLATION

FTD-ID(RS)T-0645-79 21 June 1979

MICROFICHE NR: FTD-79-C-000822

CSB78087156

COMPUTATION OF SUPERSONIC SPACE ENCIRCLING FLOW OF BLUNT-NOSED BODY

By: Zhu Youlan, Wang Ruquan, Zhong Xichang

English pages: 27

Source: Li Hsueh, Nr. 4, 1977, pp. 270-282

Country of Origin: China
Translated by: LINGUISTIC SYSTEMS, INC.
F33657-78-D-0618
H. P. Lee
Requester: FTD/TQTA

Computation of Supersonic Space Encircling Flow of Blunt-Nosed Body

Zhu Youlan, Wang Ruquan, Zhong Xichang

Computer Technology Research Institute
The Chinese Academy of Science

Contents

Research Report

Computation of Supersonic Space Encircling Flow of Blunt-Nosed Body

Zhu Youlan, Wang Ruquan, Zhong Xichang

Computer Technology Research Institute
The Chinese Academy of Sciences

I. Introduction

Since the 1950's, for numerical solution of the problems of supersonic inviscid encircling flow of blunt-nosed body, a number of different methods has been developed. Of them one category is stationary method and the other is nonstationary method. In the category of stationary method, there are method of finite difference, method of integral relation and method of lines. Applied to smooth bodies, all these methods can have satisfactory results. Only because the nonstationary method must take steady process for time, it has to consume a great deal of machine time. As for the method of finite difference, in order to have very precise result, it needs quite a number of net points and large machine storage capacity, and it uses more computing time. Compared with these conditions, the method of lines has more points of excellence. For instance, its computing method is simple, the storage capacity it needs is small and, using only a few rays, it can bring about satisfactory result. This article is intended to report our work of using the method of lines to compute supersonic encircling flow of blunt-nosed body.

We use the method of lines to make broad computation of supersonic

encircling flow of blunt-nosed body. The objects we computed include ellipsoid of various axial ratio and disk-analogue bodies. The range of incoming flow M number is 1.5 to infinity. Under the condition of axial symmetry, besides the frozen gas of $\gamma = 1.4$, we have also computed balanced and unbalanced air.

In addition, we ,too, use the method of lines to compute the flow in supersonic zone and the pointed conical encircling flow with attack angle.

To the results of computation, we make multi-way check, and all show that the results of computation by using method of lines are considerably satisfactory.

2. The Way of Relaying Questions

2.1 Fundamental Equation

To consider the inviscid and non-heat conducting air flow. The equation of aerodynamics in spherical coordinate system (r, θ, φ) is:

$$\left.\begin{aligned}
&\frac{1}{r^2\sin\theta}\left\{\frac{\partial}{\partial r}(\rho u r^2\sin\theta)+\frac{\partial}{\partial\theta}(\rho v r\sin\theta)+\frac{\partial}{\partial\varphi}(\rho w r)\right\}=0\\
&\frac{du}{dt}-\frac{v^2+w^2}{r}+\frac{1}{\rho}\frac{\partial p}{\partial r}=0\\
&\frac{dv}{dt}+\frac{uv}{r}-\frac{\operatorname{ctg}\theta}{r}w^2+\frac{1}{r\rho}\frac{\partial p}{\partial\theta}=0\\
&\frac{dw}{dt}+\frac{uw}{r}+\frac{\operatorname{ctg}\theta}{r}vw+\frac{1}{\rho r\sin\theta}\frac{\partial p}{\partial\varphi}=0\\
&\frac{dp}{dt}-c^2\frac{d\rho}{dt}=0
\end{aligned}\right\} \qquad (2.1)$$

Here $\frac{d}{dt} = u\frac{\partial}{\partial r} + v\frac{1}{r}\frac{\partial}{\partial \theta} + w\frac{1}{r\sin\theta}\frac{\partial}{\partial \varphi}$, u, v, w are component when speed is along r, θ, φ direction, p is pressure, p is density and c is speed. In the equation, all quanity are dimensionless quantity and their dimension factor are respcetively

$$p \sim \rho_\infty V_\infty^2, \quad \rho \sim \rho_\infty, \quad u, v, w \sim V_\infty, \quad r \sim R_0$$

Here ∞ indicates the quanity of incoming flow and R_0 is the curvature radius at the top of the subject.

For the convenience of computing, we introduce the following transformation of coordinate,

$$\xi = \frac{r - G(\theta, \varphi)}{F(\theta, \varphi) - G(\theta, \varphi)}, \quad \theta = \theta, \quad \varphi = \varphi$$

Here $r = G(\theta, \varphi)$ & $r = F(\theta, \varphi)$ are equations respectively of the object surface and shock wave. Obviously, in (ξ, θ, φ) coordinate system, the shock wave is in the plane of $\xi = 1$ and the surface of the object is in the plane of $\xi = 0$. Let

$$\alpha = -(G_\theta + \xi\varepsilon_\theta), \quad \beta = -\frac{1}{\sin\theta}(G_\varphi + \xi\varepsilon_\varphi), \quad \varepsilon = F - G$$

Due to

$$\frac{\partial}{\partial r} = \frac{1}{\varepsilon}\frac{\partial}{\partial \xi}, \quad \frac{\partial}{\partial \theta} = \frac{\alpha}{\varepsilon}\frac{\partial}{\partial \xi} + \frac{\partial}{\partial \theta}$$

$$\frac{1}{\sin\theta}\frac{\partial}{\partial \varphi} = \frac{\beta}{\varepsilon}\frac{\partial}{\partial \xi} + \frac{1}{\sin\theta}\frac{\partial}{\partial \varphi}$$

so equation (2.1) can be rewritten into

$$\left.\begin{aligned} &\alpha\frac{\partial \rho}{\partial \xi} + \rho\left(r\frac{\partial u}{\partial \xi} + \alpha\frac{\partial v}{\partial \xi} + \beta\frac{\partial w}{\partial \xi}\right) = F_1, \quad \alpha\frac{\partial u}{\partial \xi} + \frac{r}{\rho}\frac{\partial p}{\partial \xi} = F_2 \\ &-\alpha\frac{\partial v}{\partial \xi} + \frac{\alpha}{\rho}\frac{\partial p}{\partial \xi} = F_3, \quad \alpha\frac{\partial w}{\partial \xi} + \frac{\beta}{\rho}\frac{\partial p}{\partial \xi} = F_4, \quad \alpha\left(\frac{\partial \rho}{\partial \xi} - c^2\frac{\partial \rho}{\partial \xi}\right) = F_5 \end{aligned}\right\} \qquad (2.2)$$

Or written into solved form of $\frac{\partial p}{\partial \xi}, \cdots, \frac{\partial w}{\partial \xi}$

$$\left.\begin{aligned}
\frac{\partial p}{\partial \xi} &= \frac{c^2[F_1 a - \rho(\tau F_2 + \alpha F_3 + \beta F_4)] + F_5 a}{a^2 - \tau^2 c^2} \\
\frac{\partial \rho}{\partial \xi} &= \frac{1}{c^2}\left[-\frac{F_5}{a} + \frac{\partial p}{\partial \xi}\right] \\
\frac{\partial u}{\partial \xi} &= \frac{1}{a}\left[F_2 - \frac{\tau}{\rho}\frac{\partial p}{\partial \xi}\right] \\
\frac{\partial v}{\partial \xi} &= \frac{1}{a}\left[F_3 - \frac{\alpha}{\rho}\frac{\partial p}{\partial \xi}\right] \\
\frac{\partial w}{\partial \xi} &= \frac{1}{a}\left[F_4 - \frac{\beta}{\rho}\frac{\partial p}{\partial \xi}\right]
\end{aligned}\right\} \qquad (2.3)$$

In the equation, $a = u\tau + v\alpha + w\beta$

$$\tau^2 = \tau^2 + \alpha^2 + \beta^2$$

$$F_1 = -\varepsilon\left\{v\frac{\partial \rho}{\partial \theta} + \frac{w}{\sin\theta}\frac{\partial \rho}{\partial \varphi} + \rho\left[2u + \frac{\partial v}{\partial \theta} + \frac{1}{\sin\theta}\left(v\cos\theta + \frac{\partial w}{\partial \varphi}\right)\right]\right\}$$

$$F_2 = -\varepsilon\left[v\frac{\partial u}{\partial \theta} + \frac{w}{\sin\theta}\frac{\partial u}{\partial \varphi} + (v^2 + w^2)\right]$$

$$F_3 = -\varepsilon\left[v\left(\frac{\partial v}{\partial \theta} + u\right) + \frac{w}{\sin\theta}\left(\frac{\partial v}{\partial \varphi} - \cos\theta w\right) + \frac{1}{\rho}\frac{\partial p}{\partial \theta}\right]$$

$$F_4 = -\varepsilon\left[v\frac{\partial w}{\partial \theta} + uw + \frac{w}{\sin\theta}\left(\frac{\partial w}{\partial \varphi} + v\cos\theta\right) + \frac{1}{\rho\sin\theta}\frac{\partial p}{\partial \varphi}\right]$$

$$F_5 = -\varepsilon\left[v\left(\frac{\partial \rho}{\partial \theta} - c^2\frac{\partial \rho}{\partial \theta}\right) + \frac{w}{\sin\theta}\left(\frac{\partial \rho}{\partial \varphi} - c^2\frac{\partial \rho}{\partial \varphi}\right)\right]$$

2.2 Boundary Condition

(1) Condition of shock wave On the shock wave, the shock wave relation equation must be satisfied.

$$\left.\begin{aligned}
h + \frac{V_n^2}{2} &= h_\infty + \frac{V_{\infty n}^2}{2} \\
p + \rho V_n^2 &= p_\infty + \rho_\infty V_{\infty n}^2 \\
u &= u_\infty - \left(1 - \frac{\rho_\infty}{\rho}\right) n_1 V_{\infty n} \\
v &= v_\infty - \left(1 - \frac{\rho_\infty}{\rho}\right) n_2 V_{\infty n} \\
w &= w_\infty - \left(1 - \frac{\rho_\infty}{\rho}\right) n_3 V_{\infty n}
\end{aligned}\right\} \qquad (2.4)$$

Here the quantity indicated by an infinity mark is wave-front quantity and that not indicated by an infinity mark is wave-back quantity, V_n is the projection of $\overset{\text{speed}}{\underset{\wedge}{}}$ along the direction of wave normal line, h is han, (n_1, n_2, n_3) are direction cosin respectively along the shock wave normal line, namely

$$\begin{pmatrix} n_1 \\ n_2 \\ n_3 \end{pmatrix} = \frac{1}{\sqrt{1 + \left(\frac{F_\theta}{r}\right)^2 + \left(\frac{F_\varphi}{r \sin\theta}\right)^2}} \times \begin{pmatrix} 1 \\ -\frac{F_\theta}{r} \\ -\frac{F_\varphi}{r \sin\theta} \end{pmatrix}$$

(2) Condition of the object surface. On the surface of the object, it must satisfy the condtion that the normal direction speed is zero, namely

$$q = uG - vG_\theta - w\frac{G_\varphi}{\sin\theta} = 0 \quad (2.5)$$

3. Numerical Solution

In order to make numerical solution, we introduce some rays to the solution zone. For instance, at θ direction we introduce coordinate surface of $\theta = \theta_i = \text{const}$ and at φ direction, we introduce coordinate surface of $\varphi = \varphi_i = \text{const}$, then we take the intersecting lines of these coordinate surfaces as rays. Fors, we use the value of flow parametre on the ray as nodal point value to construct interpolating polynomial equation and then to

determine the partial derivative of θ & φ correspondingly. Let equation (2.3) be formulated on the ray, then we have a constant differential equation group and the problem of marginal value will correspondingly become marginal-value problem of constant differential equation group. For this reason, we change marginal-value problem into initial-value problem, and work out solution through iteration, namely we first assume that the form of shock wave has been known, and, then from shock wave condition (2.4), we have the flow parametre of wave-back. Taking this as initial value of integral constant differential equation group, then we check whether the flow parametre of the object surface can satisfy the condition of object surface (2.5). If not, we adjust the shape of shock wave till the condition of object surface is satisfied. The integration of constant differential equation can use general method, such as quartric-valence Runge-Kutta method. In the following, we shall describe some specific treatment.

3.1 Equation on Axis $\theta = 0$

Assuming that flow field is symmetrical with $\varphi = 0$, $*$ plane and that axis $\theta = 0$ is always in a symmetrical plane. From equation (2.2), it can be seen that due to the fact that $\sin\theta$ appears in the denominator, the equation at $\theta = 0$ must be given a treatment. Let $v^* = v(\xi, 0, 0)$, clearly $v(\xi, 0, \varphi) = v^*(\xi)\cos\varphi$, $w(\xi, 0, \varphi) = -v^*(\xi)\sin\varphi$, $u(\xi, 0, \varphi) = u(\xi, 0, 0)$, $\rho(\xi, 0, \varphi) = \rho(\xi, 0, 0)$, $\rho(\xi, 0, \varphi) = \rho(\xi, 0, 0)$. By applying Low-bi-ta (transliteration of Chinese sound and it may be a Chinese transliteration of Robert) method to o/o which appears in equation (2.2), we can have the equation on $\theta = 0$. In principle, it will do by taking any equation from φ surface randomly. But because the

computing error of numerical value, of different φ, there will be different results. In order to eliminate such incongruity, we make integration of those equations of φ from $0 - \pi$ to induce the necessary equation. For instanec, we use $\cos\varphi$ to multiply the third equation of equation (2.2), and take off the fourth equation and use $\sin\varphi$ to multiply it, then we make integration. Due to

$$\int_0^{\pi} a\left(\frac{\partial v}{\partial \xi}\cos\varphi - \frac{\partial w}{\partial \xi}\sin\varphi\right)d\varphi - \int_0^{\pi}(ru + \alpha v + \beta w)\frac{\partial v^*}{\partial \xi}d\varphi = a^*\frac{\partial v^*}{\partial \xi}$$

$$\frac{1}{\rho}\int_0^{\pi}(\alpha\cos\varphi - \alpha_\varphi\sin\varphi)\frac{\partial p}{\partial \xi}d\varphi = \frac{\pi}{\rho}\frac{\partial p}{\partial \xi}$$

$$\frac{1}{\pi}\int_0^{\pi}(F_3\cos\varphi - F_4\sin\varphi)d\varphi = -\frac{2\varepsilon}{\pi}\left\{\int_0^{\pi}\left[v^*\left(\frac{\partial v}{\partial \theta}\cos^2\varphi - \frac{\partial w}{\partial \theta}\sin\varphi\cos\varphi\right)\right.\right.$$

$$\left.\left. + \frac{1}{\rho}\frac{\partial p}{\partial \theta}\cos\varphi\right]d\varphi + \frac{\pi}{2}uv^*\right\} - F_3^*$$

So we can have

$$a^*\frac{\partial v^*}{\partial \xi} + \frac{\alpha^*}{\rho}\frac{\partial p}{\partial \xi} - F_3^*$$

And analogously we can have

$$a^*\frac{\partial u}{\partial \xi} + \frac{r}{\rho}\frac{\partial p}{\partial \xi} - F_2^*$$

$$a^*\frac{\partial p}{\partial \xi} + \rho\left(\frac{\partial u}{\partial \xi} + \alpha^*\frac{\partial v^*}{\partial \xi}\right) - F_1^*$$

$$a^*\left(\frac{\partial p}{\partial \xi} - c^2\frac{\partial \rho}{\partial \xi}\right) - F_3^*$$

To write into solved form of $\frac{\partial p}{\partial \xi}, \cdots, \frac{\partial v^*}{\partial \xi}$, we can have the necessary equation

$$\left.\begin{aligned}
\frac{\partial p}{\partial \xi} &= \frac{c^2[F_1^*a^* - \rho(rF_2^* + \alpha^*F_3^*)] + a^*F_3^*}{a^{*2} - \tau^{*2}c^2}\\
\frac{\partial \rho}{\partial \xi} &= \frac{1}{c^2}\left[-\frac{F_3^*}{a^*} + \frac{\partial p}{\partial \xi}\right]\\
\frac{\partial u}{\partial \xi} &= \frac{1}{a^*}\left[F_2^* - \frac{r}{\rho}\frac{\partial p}{\partial \xi}\right]\\
\frac{\partial v^*}{\partial \xi} &= \frac{1}{a^*}\left[F_3^* - \frac{\alpha^*}{\rho}\frac{\partial p}{\partial \xi}\right]
\end{aligned}\right\} \qquad (2.6)$$

In it,

$$a^* = \frac{2}{\pi}\int_0^{\pi} a\cos\varphi d\varphi$$

$$a^* = ru + a^* v^*$$

$$\tau^{*2} = r^2 + a^{*2}$$

$$F_1^* = -\frac{2\varepsilon}{\pi}\left\{v^*\int_0^{\pi}\frac{\partial\rho}{\partial\theta}\cos\varphi d\varphi + \rho\int_0^{\pi}\frac{\partial v}{\partial\theta}d\varphi + \rho u\pi\right\}$$

$$F_2^* = -\frac{2\varepsilon}{\pi}\left\{v^*\int_0^{\pi}\frac{\partial u}{\partial\theta}\cos\varphi d\varphi - \frac{\pi}{2}v^{*2}\right\}$$

$$F_3^* = -\frac{2\varepsilon}{\pi}\left\{\int_0^{\pi}\left[v^*\left(\frac{\partial v}{\partial\theta}\cos^2\varphi - \frac{\partial w}{\partial\theta}\sin\varphi\cos\varphi\right) + \frac{1}{\rho}\frac{\partial\rho}{\partial\theta}\cos\varphi\right]d\varphi + \frac{\pi}{2}uv^*\right\}$$

$$F_5^* = -\frac{2\varepsilon}{\pi}v^*\int_0^{\pi}\left(\frac{\partial\rho}{\partial\theta} - c^2\frac{\partial\rho}{\partial\theta}\right)\cos\varphi d\varphi$$

3.2 Interpolating Multinomial Equation

Because the flow field is assumed to be symmetrical with $\varphi = 0, \pi$ plane, it is only necessary to have solution between $0 \leqslant \varphi \leqslant \pi$. Between $0-\pi$, we introduce $k+1$ planes. And at the same time, we make n + 1 conical surfaces, $\theta = \theta_k = \text{const}\ (\theta_0 = 0)$, $k = 0, 1, \ldots,$ n. They intersect with half plane $\varphi = \varphi_i$ and $\varphi = \varphi_i + \pi$ to form (2n + 1) rays. Noticing that the flow parametre on the flow symmetry, $\varphi = \pi - \varphi_i$ and the flow parametre on $\varphi = \varphi_i + \pi$ are equal or different by one symbol, for the fixed ξ, we can utilize the value of 2n + 1 rays on $\varphi = \varphi_i$ & $\varphi = \pi - \varphi_i$ to construct 2nth order interpolating multinomial equation of θ.

$$g = \sum_{i=0}^{2n} a_i\theta^i \qquad (2.7)$$

g indicates flow parametre. For the purpose of saving time in the process of computing, we do not first compute coefficient a_i, but use the following computing methods instead. Because interpolating function and its derivate

can be expressed as a linear combination of function values on interpolating nodal point, and the linear combination coefficient is only related with the position of interpolating nodal point and the position of interpolating point, so when the nodal point and interpolating point are given, these coefficients can be determined. When the function of each point and the derivate value are computed, it will do to use these coefficients and the function value on nodal point to make point product. Taking equation (2.7) as example. If nodal point is $\theta_m (m = 0, 1, \cdots, 2n)$, $g(\theta)$ at θ of some interpolating point will be computed. Because there is condition at nodal point,

$$\sum_{i=0}^{2n} a_i \theta_m^i = g_m \quad (m = 0, 1, \cdots, 2n)$$

$g_m = g(\theta_m)$. or written into matrix form:

$$M\mathbf{a} = \mathbf{g}$$

Here

$$M = \begin{pmatrix} 1 & \theta_0 & \theta_0^2 \cdots\cdots & \theta_0^{2n} \\ 1 & \theta_1 \cdots\cdots & & \theta_1^{2n} \\ \cdots\cdots & & & \\ 1 & \theta_{2n} \cdots\cdots & & \theta_{2n}^{2n} \end{pmatrix}$$

$$\mathbf{a} = \begin{pmatrix} a_0 \\ a_1 \\ \vdots \\ a_{2n} \end{pmatrix} \quad \mathbf{g} = \begin{pmatrix} g_0 \\ g_1 \\ \vdots \\ g_{2n} \end{pmatrix}$$

Therefore we have

$$\mathbf{a} = M^{-1}\mathbf{g}$$

Then we can rewrite the equation of $g(\theta)$,

$$g(\theta) = \mathbf{d}^* \cdot \mathbf{a}$$

Into

$$\begin{aligned} g(\theta) &= \mathbf{d}^* \cdot (M^{-1}\mathbf{g}) \\ &= (M^{-1*}\mathbf{d})^* \cdot \mathbf{g} \\ &= \mathbf{b}^* \cdot \mathbf{g} \end{aligned} \qquad (2.8)$$

Here $\mathbf{b} = M^{-1*}\mathbf{d}$, & $\mathbf{d}^* = (1, \theta, \cdots, \theta^{2n})$. Evidently, when nodal point and interpolating point are given, M* and **d** can be determined and then we can have b. Similarly because,

$$\begin{aligned} g'_\theta(\theta) &= \sum_{i=0}^{2n} a_i i(\eta)^{i-1} \\ &= \mathbf{d}_1^* \cdot \mathbf{a} \\ &= (M^{*-1}\mathbf{d}_1)^* \cdot \mathbf{g} \end{aligned}$$

Here $\mathbf{d}_1^* = (0, 1, 2\theta, \cdots, 2n\theta^{2n-1})$, represents derivate of θ, so to compute derivate can be of an analogous treatment.

So far as φ is concerned, when θ is fixed, we can utilize the value at its intersecting line with $k+1$ planes to construct trigonometric interpolating multinomial equation of φ. In computing, the method mentioned above can also be used. For even function, we take,

$$g = \sum_{i=0}^{k} a_i \cos^i \varphi$$

Then

$$g'_\varphi = (M^{*-1}\mathbf{d}_1)^* \cdot \mathbf{g}$$

Now there is

$$M^* = \begin{pmatrix} 1 & 1 & \cdots & 1 \\ \cos\varphi_0 & \cos\varphi_1 & \cdots & \cos\varphi_k \\ \vdots & \vdots & \cdots & \vdots \\ \cos^k\varphi_0 & \cos^k\varphi_1 & \cdots & \cos^k\varphi_k \end{pmatrix}$$

$$\mathbf{d}_1^* = (0, -\sin\varphi, \cdots, -k\sin\varphi\cos^{k-1}\varphi)$$

$$\mathbf{g}^* = (g_0, g_1, \cdots, g_k)$$

For $\frac{1}{\pi}\int_0^{\pi} g\,d\varphi$, $\frac{1}{\pi}\int_0^{\pi} g\cos\varphi\,d\varphi$, similar expression can also be written.It is not necrssary to examplify them here. For odd function, we take,

$$g = \sum_{i=0}^{k-2} a_i \cos^i\varphi \sin\varphi$$

Then

$$g'_k = (M^{*-1}\mathbf{d}_1)^* g$$

Now

$$M^* = \begin{pmatrix} \sin\varphi_1 & \sin\varphi_2 \cdots\cdots\cdots\cdots \sin\varphi_{k-1} \\ \sin\varphi_1\cos\varphi_1 & \vdots \qquad\qquad\qquad \vdots \\ \vdots & \vdots \qquad\qquad\qquad \vdots \\ \sin\varphi_1\cos^{k-2}\varphi_1 & \sin\varphi_2\cos^{k-2}\varphi_2 \cdots \sin\varphi_{k-1}\cos^{k-2}\varphi_{k-1} \end{pmatrix}$$

$$\mathbf{d}_1^* = (\cos\varphi, -\sin^2\varphi + \cos^2\varphi, \cdots, (k-2)\cos^{k-1}\varphi\sin^2\varphi + \cos^{k-1}\varphi)$$

In addition to the methods mentioned above, we also use the following methods to construct interpolating multinomial equations. For even function of φ , we take

$$g(\xi) = \sum_{i=0}^{n} \sum_{j=0}^{k} g_{ij}(\xi)\theta^i \cos^j\varphi$$

For odd function, we take

$$\omega(\xi) = \left(\sum_{i=0}^{n} \sum_{j=0}^{k} \omega_{ij}(\xi)\theta^i \cos^j\varphi\right) \sin\varphi$$

In order to make the function and the derivate of θ at $\theta = 0$ in some sense be single value, some proper condition must be added to the multinomial equation. Now we try to describe such conditions.

For instance, for shock wave form, $r = F(\theta, \varphi)$, we naturally require, when $\theta = 0$, it has no relationship with φ. This means that we require when $j \neq 0$, $F_{0j} = 0$. And at the same time, in order to warrant that the normal

line has definite direction and when $\theta = 0$, the normal line direction spherical coordinate should have such a form: $(a, b\cos\varphi, -b\sin\varphi)$ and in it a and b are constants. This means to require $F_{ij} = 0\,(j \neq 1)$. So for F, the multinomial equation should be:

$$F(\theta, \varphi) = F_{00} + F_{11}\theta\cos\varphi + \sum_{i=2}^{n}\sum_{j=0}^{k} F_{ij}\theta^i\cos^j\varphi \tag{2.9}$$

Obviously, u,p, and ρ should also have the same form as F. The above conclusion and the form of v and w can be obtained as well in the following way. Let

$$g = g_{00}(\xi) + \sum_{i=1}^{n}\sum_{j=0}^{k} g_{ij}(\xi)\theta^i\cos^j\varphi$$

$$v = v_{01}(\xi)\cos\varphi + \sum_{i=1}^{n}\sum_{j=0}^{k} v_{ij}(\xi)\theta^i\cos^j\varphi$$

$$w = -v_{01}(\xi)\sin\varphi + \left(\sum_{i=1}^{n}\sum_{j=0}^{k} w_{ij}(\xi)\theta^i\cos^j\varphi\right)\sin\varphi$$

Here g can be used to express p,ρ,u,F, and utilizes the property $v(\xi, 0, \varphi) = A\cos\varphi$, $w(\xi, 0, \varphi) = -A\sin\varphi$, then there is $v_{0j} = 0\,(j \neq 1)$, $w_{0j} = 0(j \neq 0)$, $v_{01} = -w_{00}$. To combine the above equation with equation (2.2),we notice that,

$$\frac{\partial}{\partial\theta}G(0, \varphi) = G_\theta(0, 0)\cos\varphi,$$

$$\frac{G_\varphi}{\sin\theta}\Big|_{\theta=0} = -G_\theta(0, 0)\sin\varphi$$

(Here the object body is symmetrical with $\varphi = 0, \pi$ surface), so when $\theta \to 0$, we have

$$a_0\frac{d\rho_{00}}{d\xi} + r_0\rho_{00}\frac{du_{00}}{d\xi} - \rho_{00}[G_{\theta 0} + \xi(F_{11} - G_{\theta 0})]\frac{dv_{01}}{d\xi} = \lim_{\theta\to 0} F_1$$

$$a_0\frac{du_{00}}{d\xi} + \frac{r_0}{\rho_{00}}\frac{dp_{00}}{d\xi} = \lim_{\theta\to 0} F_2$$

$$\left(a_0\frac{dv_{01}}{d\xi}-\frac{G_{\theta 0}+\xi(F_{11}-G_{\theta 0})}{\rho_{00}}\frac{dp_{00}}{d\xi}\right)\cos\varphi=\lim_{\theta\to 0}F_3$$

$$-\left(a_0\frac{dv_{01}}{d\xi}-\frac{G_{\theta 0}+\xi(F_{11}-G_{\theta 0})}{\rho_{00}}\frac{dp_{00}}{d\xi}\right)\sin\varphi=\lim_{\theta\to 0}F_4$$

$$a_0\left(\frac{dp_{00}}{d\xi}-c_0^2\frac{d\rho_{00}}{d\xi}\right)=\lim_{\theta\to 0}F_5$$

In it

$$a_0=u_{00}r_0-v_{01}[G_{\theta 0}+\xi(F_{11}-G_{\theta 0})]$$

$$r_0=G(0,0)+\xi[F_{00}-G(0,0)]$$

$$G_{\theta 0}=\frac{\partial}{\partial\theta}G(0,0)$$

$$c_0^2=\frac{\gamma p_{00}}{\rho_{00}}$$

To write the right end of the above equation into multinomial equation of $\cos\varphi$ (or, in addition, to multiply it by $\sin\varphi$), and to use the linear independence of $1, \cos\varphi, \cdots, \cos^k\varphi$, we can reason out that g should have the form of equation (2.9) and v and w should take,

$$v=v_{01}\cos\varphi+v_{10}\theta+v_{12}\theta^2\cos^2\varphi+\sum_{i=2}^{n}\sum_{j=0}^{k}v_{ij}\theta^i\cos^j\varphi$$

$$w=-v_{01}\sin\varphi-v_{12}\theta\cos\varphi\sin\varphi+\left(\sum_{i=2}^{n}\sum_{j=0}^{k}w_{ij}\theta^i\cos^j\varphi\right)\sin\varphi$$

At the same time, we have equation on $\theta = 0$:

$$\left.\begin{aligned}
&a_0\frac{d\rho_{00}}{d\xi}+r_0\rho_{00}\frac{du_{00}}{d\xi}-\rho_{00}[G_{\theta 0}+\xi(F_{11}-G_{\theta 0})]\frac{dv_{01}}{d\xi}\\
&\quad=-(F_{00}-G(0,0))[v_{01}\rho_{11}+\rho_{00}(v_{12}+2v_{10}+2u_{00})]\\
&a_0\frac{du_{00}}{d\xi}+\frac{r_0}{\rho_{00}}\frac{dp_{00}}{d\xi}=-(F_{00}-G(0,0))v_{01}(u_{11}-v_{01})\\
&a_0\frac{dv_{01}}{d\xi}-\frac{G_{\theta 0}+\xi(F_{11}-G_{\theta 0})}{\rho_{00}}\frac{dp_{00}}{d\xi}\\
&\quad=-(F_{00}-G(0,0))\left[v_{01}(v_{10}+v_{12}+u_{00})+\frac{p_{11}}{\rho_{00}}\right]\\
&a_0\left(\frac{dp_{00}}{d\xi}-c_0^2\frac{d\rho_{00}}{d\xi}\right)=-(F_{00}-G(0,0))v_{01}\left(p_{11}-\frac{\gamma p_{00}}{\rho_{00}}\rho_{11}\right)
\end{aligned}\right\}\qquad(2.10)$$

3.3 Iteration Method

As what has been stated at the beginning of this section, we shall try to solve the problem of marginal value through iteration. In fact, it can be interpreted as a problem of solving a transcendental equation group. That is to select one group of F_i (to indicate the shock wave form on ith ray). To make,

$$q_j(F_1, \cdots, F_m) = 0 \quad (j = 1, 2, \cdots, m)$$

Here $q_j = 0$ is the boundary condition (2.5). We use Newton method, namely to use alteration quantity δF_i of F_i to satisfy the following equation:

$$\sum_{i=0}^{m} \frac{\partial q_j}{\partial F_i} \delta F_i = -q_j \quad (j = 1, \cdots, m)$$

Usually there is no way to express partial derivate $\frac{\partial q_j}{\partial F_i}$ by using analytic equation, so we use numerical value method, namely

$$\frac{\partial q_j}{\partial F_i} = \frac{q_j(F_1, \cdots, F_{i-1}, F_i + \Delta F_i, F_{i+1}, \cdots, F_m) - S_j(F_1, \cdots, F_m)}{\Delta F_i}$$

By using this method, it needs m + 1 times of integration for each iteration, so it consumes a great deal of machine time. For the purpose of saving time, we can use the simplified Newton method, but because of the lack of accuracy in msot of $\frac{\partial q_j}{\partial F_i}$, the speed of convergence, therefore, can possibly become slow. In order to make $\frac{\partial q_j}{\partial F_i}$ more accurate without increasing much of the volume of computation, we suggest a method as follows. Let Q indicate the vector constructed from $q_1, \cdots, q_m$. R is the vector constructed from F_1, ..., F_m. Q' is derivative index of Q to R. If $Q(R_0) = Q_0$, and at other m-point of R_1, ..., R_m, close to R_0, $Q(R_i) = Q_i (i = 1, \ldots, m)$ has been known, and if $R_0 - R_i (i = 1, 2, \ldots, m)$ is linear independent, then Q'_0 can be decided

approximately by R_i and Q_i. In fact, because

$$Q_i \approx Q_0 + Q_0'(R_i - R_0) \quad (i = 1, 2, \cdots, m)$$

So there is

$$(Q_1 - Q_0, \cdots, Q_m - Q_0) \approx Q_0'(R_1 - R_0, \cdots, R_m - R_0)$$

and then there is

$$Q_0' \approx (Q_1 - Q_0, \cdots, Q_m - Q_0)(R_1 - R_0, \cdots, R_m - R_0)^{-1}$$

thus we can have an iteration formula

$$R_{n+1} = R_n - (R_{n-m} - R_n, \cdots, R_{n-1} - R_n)(Q_{n-m} - Q_n, \cdots, Q_{n-1} - Q_n)^{-1}Q_n'$$
$$n = m + 1, \cdots \tag{2.11}$$

Evidently, using the above equation to make iteration and begin with R_1, ..., R_{m+1} to solve $Q_1, \cdots, Q_{m+1}$ needs m + 1 times of integration. But thereafter, one iteration needs only one time of integration.

Now we try to make a simple estimation of the speed of convergence. Obviously, when

$$\tilde{R}_{m+1} \equiv (R_1 - R_{m+1}, \cdots, R_m - R_{m+1}) = \Delta F \cdot E$$

equation (2.11) becomes difference half Newton formula. Here E is unit matrix and ΔF is pure quanty. Because now there is,

$$\tilde{Q}_{m+1} \equiv (Q_1 - Q_{m+1}, \cdots, Q_m - Q_{m+1}) = Q_{m+1}'\tilde{R}_{m+1} + o(\Delta F^2)$$

Then there is

$$Q_{m+1}'^{-1} = \tilde{R}_{m+1}\tilde{Q}_{m+1}^{-1} + o(\Delta F^2)\tilde{Q}_{m+1}^{-1} = \tilde{R}_{m+1}\tilde{Q}_{m+1}^{-1} + o(\Delta F)$$

And thereupon we can have an estimation equation for difference half Newton formula.

$$\begin{aligned} R^* - R_{m+2} &= R^* - R_{m+1} + \tilde{R}_{m+1}\tilde{Q}_{m+1}^{-1}Q_{m+1} \\ &= R^* - R_{m+1} + Q_{m+1}'^{-1}Q_{m+1} + (\tilde{R}_{m+1}\tilde{Q}_{m+1}^{-1} - Q_{m+1}'^{-1})Q_{m+1} \\ &= o(\|R^* - R_{m+1}\|^2) + o(\Delta F\|Q_{m+1}\|) \end{aligned}$$

or written into

$$\|R^* - R_n\| \leqslant A\|R^* - R_{n-1}\|^2 + B\Delta F\|Q_{n-1}\| \quad (n = 1, 2, \cdots)$$

Here R* is true solution, $\|\ \|$ indicates mode, and A and B are suitable constants. Similarly, for difference simplified Newton method, there is an estimation equation,

$$\|R^* - R_n\| \leqslant A\|R^* - R_{n-1}\| + B\Delta F\|Q_{n-1}\| + C\|R_{m+1} - R_{n-1}\|\|Q_{n-1}\|$$
$$(n = m + 2, \cdots)$$

For the method suggested by us there is an estimation equation,

$$\|R^* - R_n\| \leqslant A\|R^* - R_{n-1}\| + D\|\tilde{Q}_{n-1}^{-1}\| \sup_{1<i<n}\|R_{n-1} - R_{n-i-1}\|^2\|Q_{n-1}\|$$

Here A, B, C, and D are constants.

It is easy to see that when ΔF & $\|R^* - R_{n-1}\|$ are of same quantity level or smaller, difference Newton method basically maintains the speed of convergence of Newton method. But $\|R_{m+1} - R_{n-1}\|$ is generally increased as n is increased, so of simplified Newton method the speed of convergence is slow. Because $\|\tilde{Q}_{m-1}^{-1}\| \sup_{1<i<n}\|R_{n-1} - R_{n-i-1}\| = o(1)$, and $\sup_{1<i<n}\|R_{n-1} - R_{n-i-1}\|$ is reduced as n is increased, so the method suggested by us can possibly converge faster than simplified Newton method. This has been proved in practical computation.

3.4 Selection of Initial Shock Wave and Interpolation of Object Surface Quantity

When the methods mentioned above are used to make iteration, the success in computing will depend on how well the selection of initial shock wave is made . For this reason, we use the ready results according to the way of some parametre gradual transition. For instance, when we want to compute

the flow result under certain attack angle η^*, we select attack angle η as parametre. After the result of η_0 has been obtained (for example $\eta_0 = 0^0$), the result can be used as initial value to compute $\eta_0 + \Delta\eta$. After we have had the result of $\eta_0 + \Delta\eta$, we use the results of η_0, $\eta_0 + \Delta\eta$ to obtain initial value of $\eta_0 + 2\Delta\eta$ by way of linear interpolation. In the same fashion, till we have the result of η^*. As for the initial shock wave form which is needed in the beginning of computing, it can be secured by utilizing the result available currently.

From equation (2.3), it can be understood that on the object surface $a = 0$, so integration cannot reach the object surface. In order to have the quantity of object surface, we use extrapolation method. When integration reaches a certain ξ^*(for example $\xi^* = 0.1$), then we use the ξ values of a few neighbouring points to extrapolate the object surface quantity for example using the values of $\xi = 0.3, 0.2, 0.1$ makes a quadratic interpolation. Here we would like to make a random suggestion that if the other computing form, such as implicit form integration, extrapolation can be completely avoided. For a situation of axial symmetry, we designed another form to compute, and the result proves that it is a success. Here we have no plan to give its details.

4. Computation Results

We have made broad computation on blunt-nosed body, axial symmetry and three-dimension space encirling flows by using the methods mentioned above. The object forms we computed include ellipsoid of various axial ratio and objects analogous to disk (object expressed by equation $z^n + (x^2 + y^2)^{n/2} = 1^n$,

$n \geq 2$). The range of incoming flow M is $1.5 \leq M_\infty \leq \infty$. For the situation of axial symmetry, besides the frozen gas of $\gamma = 1.4$, we compute the balanced air as well as the unbalanced. The method we used is borrowed from article 12 in the bibliography appended to this article. The patterns of unbalanced air are presented in another article of ours. The precision of our computation results have been checked by several different ways. One of the checks is made in computing as it is in process. For instance, we use different number of rays and different integral step length to check the relations which should be satisfied by flow field, such as maintaining constancy. Another way is to compare with other results acquired from experiments and other methods, such as integral relation method. All the checks we made indicate that the precision of our computation results is satisfactory. In the following, we shall present a part of our computation results.

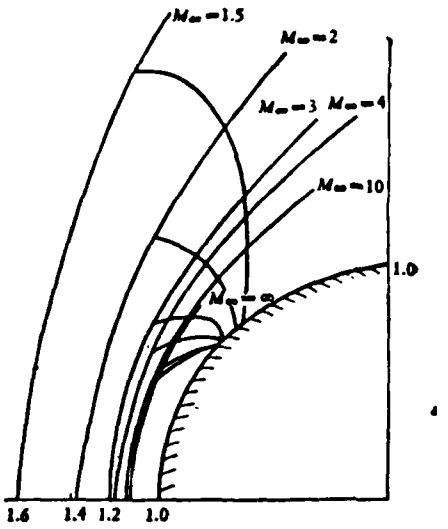

Figure 1 Forms of shock wave and sonic line of frozen gas encirling flow

Figure 1 illustrates the forms of shock wave and sonic line of frozen gas spherical flow under different M_∞ number. From the Figure, it can be understood that the forms of sonic line are of two different types. When $M > 3$, the limit characteristic line is the second family characteristic line that can reach sonic

point of the object surface. But when $M_\infty \leq 3$, the limit characteristic line is composed of the first family characteristic line (which comes from object surface) in contact with sonic line and the second family characteristic line (which comes from shock wave).

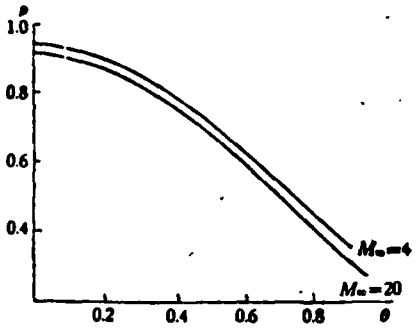

Figure 2 Distribution of pressure along object surface

Figure 2 shows the distribution of object surface pressure of frozen gas spherical flow.

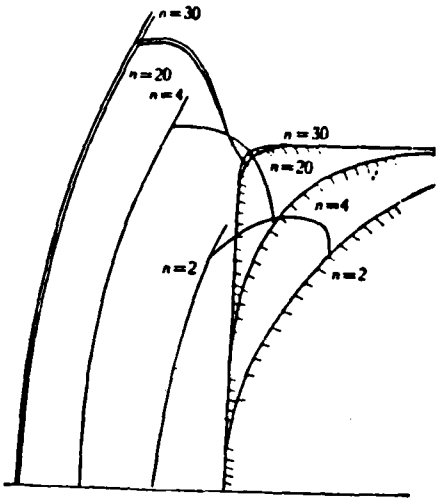

Figure 3 Shock wave position and sonic line form ($M_\infty = 3$)

Figure 3 illustrates $M_\infty = 3$, $\gamma = 1.4$, the shock wave form and sonic line position of different objects. For very blunt body, if $n \geq 20$, shock wave position will basically maintain unchanged. After the contraction of the curvature radius of object surface adjacent to sonic point, for solid M_∞ number, beginning with a certain curvature, there will be torsional point on the sonic line.

Figure 4 shows shock wave position and sonic line form of balanced air

spherical flow. The conditions of incoming flow are $M_\infty = 4$, $p_\infty = 0.87 \times 10^5$ dyne/cm^2, $\rho_\infty = 0.95 \times 10^{-4}$ g / cm ^{3} & $M_\infty = 20$, $p_\infty = 0.122 \times 10^6$ dyne/cm^2, $\rho_\infty = 0.192 \times 10^{-3}$ g/cm3. From the Figure, it can be seen that ionization

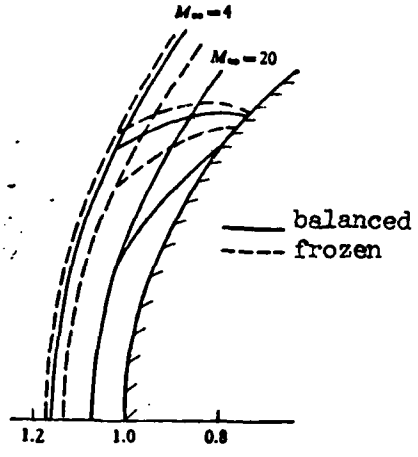

Figure 4 Form of shock wave and sonic line of balanced air spherical flow

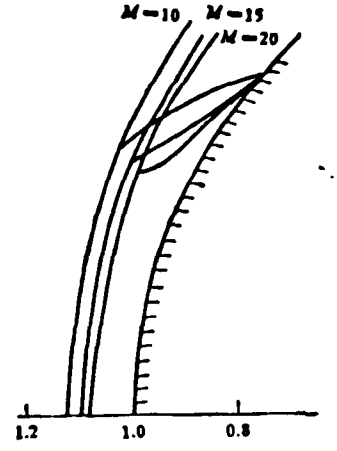

Figure 5 Form of shock wave and sonic line of unbalanced air spherical flow

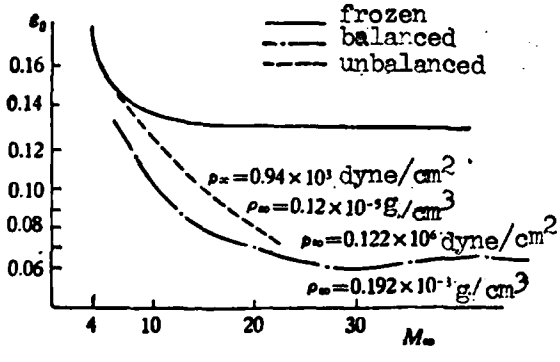

Figure 6 The detatchment distance of stationary point shock wave following M_∞ to change

makes the situation of shock wave position and sonic line with frozen gas of $\gamma = 1.4$ change remarkably. Shock wave moves much closer to the object

surface.

Figure 5 shows shock wave position and sonic line form of unbalanced air spherical flow. The conditions of incoming flow are $p_\infty = 0.947 \times 10^3$ dyne/cm^2, $\rho_\infty = 0.123 \times 10^{-3}$ g/cm^3, R = 5 cm. What is worth of attention is the special form of $M_\infty = 20$ sonic line at the place of shock wave.

Figure 6 shows the relationship between the detatchment distance of stationary point and M_∞ number. For frozen flow, when M>10, it remains unchanged. For balanced air, following the increase of M_∞, the change of detatchment distance apperas to be not unique.

Using 5 rays to compute encirling flow of axial symmetry.

Figure 7 shows that of the ellipsoidal flow of $\delta = 1.5$ when $M_\infty = 3$ & 4, shock wave and sonic line in symmetrical plane will follow the change of attack angle η. Figure 9 shows that the object surface pressure in symmetric plane will follow the change of attack angle. Also Figure 7 shows position of stationary point and, in accuracy, stationary angles of $M_\infty = 3$ & $M_\infty = 4$ are overlapping. When attack angle is changing, it moves along object surface by almost the same speed. Figure 8 shows that shock wave and sonic line in $\varphi = \pi/2$ plane follow the change of attack angle. In the Figure, it can be seen that the change of shock wave form is slow and the change of sonic line is faster.

Figure 10 shows the encirling flow of disk-analogue object of

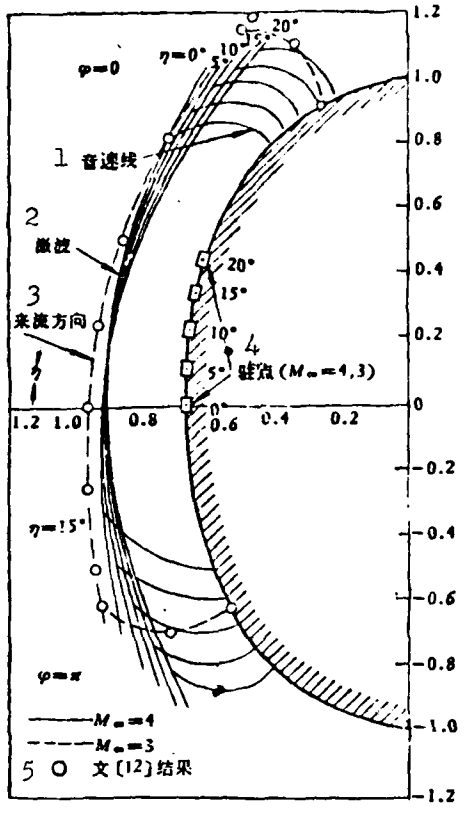

Figure 7 Shock wave form and sonic line in symmetrical plane following the change of attack angle

($\delta = 1.5$)

(1. sonic line, 2. shock wave, 3. direction of incoming flow, 4. stationary point, 5. result from article 12)

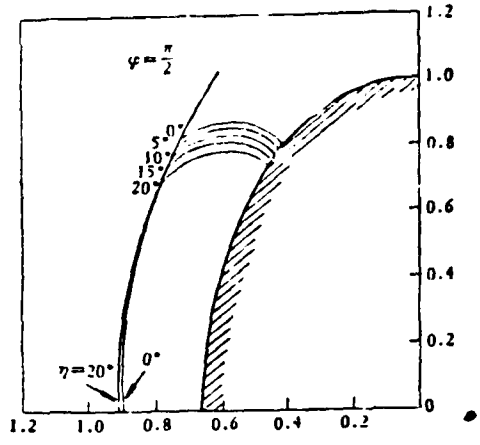

Figure 8 Shock wave form and sonic line following the change of attack angle

($M_\infty = 4$, $\delta = 1.5$)

$M_\infty = 5.8$, $n = 20$ and shock wave form and sonic line position on symmetric plane under different attack angle. Figure 11 shows the distribution of object surface pressure in symmetric plane.

When we compute space encirling flow, we take four φ surfaces and from each φ surface we take 4 rays. Because the axis line is common, we take 13 rays altogether. The z axis of coordinate system is placed in the symmetrical plane of flow field, and , for the convenience of computing, we

let it make an attack angle with angle $\bar{\beta} = (0.5—0.6)\eta$, η of the object symmetrical axis.

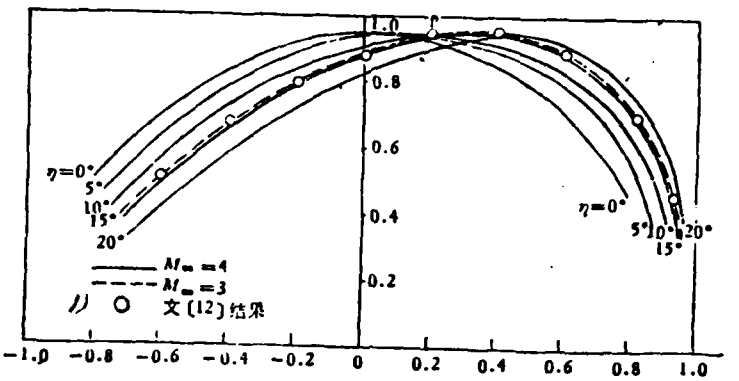

Figure 9 Object surface pressure in symmetrical plane following the change of attack angle ($\delta = 1.5$)
1) result from article 12

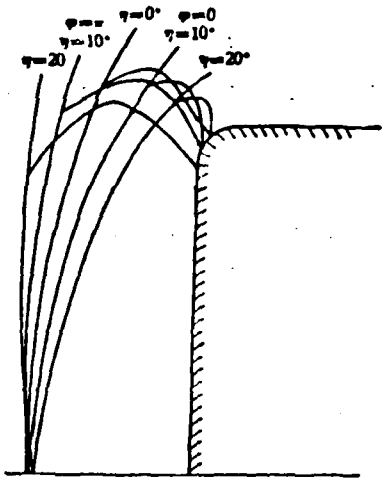

Figure 10 Shock wave form and sonic line position on symmetrical surface
($M_\infty = 5.8$, $n = 20$)

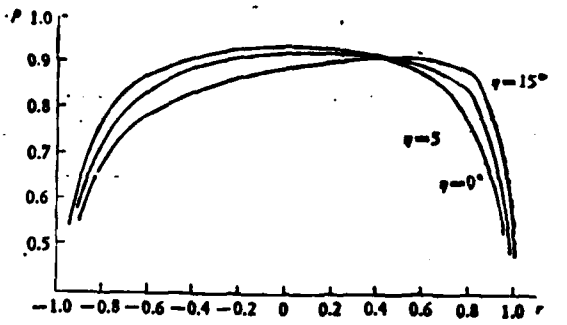

Figure 11 The distribution of object surface pressure in symmetrical surface
($M_\infty = 5.8$, $n = 20$)

About the problem of whether the greatest entropy value on object

surface can be reached, from our experience of computing, we think that for a certain object in a certain error range, the greatest entropy can be reached.

In order to check our computation results, we use several different kinds of ways. For instance, for axial symmetrical encirling flow, we use 5 rays and 3 rays respectively to compute and the result shows that error is no more than 1%. We also use different integral step length, for example, for spherical flow of $M_\infty = 6, \gamma = 1.4$, from shock wave to object surface we integrate 10-step, 20-step and 80-step. The relative error of 10-step and 20-step is no more than 0.3%, and between the results of 20-step and 80-step there are at least three same effective digits. This means that we do not have to worry about the increase of roundingoff error.

We compare the results of $M_\infty = 3, \delta = 1.5, \eta = 15^\circ$ with those of Telenin[16] they are completely identical as showed in Figure 1. For ellipsoidal and spherical frozrn flow of $\delta = 1.5$, our computation results have three coincide effective digits with the results Belotserkovskiy obtained by using integral relation method.

We also made integration check and examine the accuracy of integral equations

$$\iint_\sigma \rho \mathbf{u} \cdot d\sigma = 0$$

$$\iint_\sigma u_i \rho \mathbf{u} \cdot d\sigma + \iint_\sigma p \mathbf{x}_i \cdot d\sigma = 0$$

$$(i = 1, 2, 3)$$

$$\iint_{\sigma} p\rho^{-1}\rho \mathbf{u} \cdot d\sigma = 0$$

Here x_i indicates three axial unit vectors under rectangular coordinate, u_i is the projection of velocity vector u at three directions, σ is a curved surface containing no shock wave. Under the condition of $M_\infty = 4$, $\delta = 1.5$, and $\eta = 10°, 20°$, the integration result can be found in Table 1. Besides the total integration, Table 1 also shows the integration on shock wave,

Table 1 Integration Check $M_\infty = 4, \delta = 1.5, \beta = 0.67\eta$

η	Equation	Shock wave surface	Object surface	Conical surface	Total
10°	* Mass	−0.64327×2	0.00066×2	0.64517×2	0.00256×2
	* x方向动量	0.04595×2	−0.00731×2	−0.03849×2	0.00015×2
	y方向动量	0	0	0	0
	z方向动量	0.67039×2	−0.32282×2	−0.34862×2	−0.00105×2
	Entropy	−0.05789×2	0.00006×2	0.05809×2	0.00026×2
20°	Mass	−0.63088×2	0.00084×2	0.63298×2	0.00294×2
	* x方向动量	0.09011×2	−0.01579×2	−0.07398×2	0.00035×2
	y方向动量	0	0	0	0
	z方向动量	0.65271×2	−0.30987×2	−0.34423×2	−0.00139×2
	Entropy	−0.056379×2	0.00008×2	0.05663×2	0.00033×2

(* x,y,z direction momentum)

object surface and conical surface. From Table 1, it can be seen that the computation results are accurate, and there is error only at the third digit of the integration on shock wave and conical surface. The object surface condition is well satisfied and it is at 10^{-4} numerical level.

In addition, we also compute the total energy on all nodal points and

and entropy of each nodal point on object surface. From Table 2, it can be

Table 2 Error of Total Energy
The accuracy value of $M_\infty = 4$, $\frac{u'+v'+w'}{2} + \frac{\gamma}{\gamma-1}\frac{p}{\rho}$ is 0.65625

η	Total energy maximum deviation	Relative error
0°	0.0010	0.15%
5°	0.0019	0.30%
10°	0.0034	0.51%
15°	0.0051	0.78%
20°	0.0087	1.33%

Table 3 Entropy Value of Nodal Point on Object Surface $(\ln p - \gamma \ln \rho)$
When $M_\infty = 4$, $\delta = 1.5$, $\beta = 0.6\eta$, $\eta = 0$, the accuracy value is -2.31904

θ \ η	φ	0°	10°	20°
0°	0	-2.31903	-2.31537	-2.30611
11°	0	-2.31853	-2.31346	-2.30865
	$\frac{1}{3}\pi$		-2.31474	-2.30962
	$\frac{2}{3}\pi$		-2.31833	-2.31361
	π		-2.32091	-2.31858
22°	0	-2.31951	-2.32040	-2.32554
	$\frac{1}{3}\pi$		-2.31942	-2.32117
	$\frac{2}{3}\pi$		-2.31939	-2.31759
	π		-2.32077	-2.32111
33°	0	-2.31723	-2.31276	-2.30283
	$\frac{1}{3}\pi$		-2.31543	-2.31361
	$\frac{2}{3}\pi$		-2.31854	-2.31903
	π		-2.32045	-2.32421

seen that for $M_\infty = 4$, $\delta = 1.5$, when $\eta \leq 15°$, the relative error of total energy is less than 1%. From Table 3, it can be seen that for $M_\infty = 4$, $\delta = 1.5$, and $\eta \leq 15°$, the entropy of object surface is different only by 1 at the third effective digit, and for $\eta = 20°$, there is only a difference by 3 at the third digit.

In summary, using method of lines to compute encirling flow of smooth bodies can produce very satisfactory results.

Comrades Rui Wei-ming participated in part of this work, He Jiao-min gave us significant help, and Feng Kang once enthusiastically led us to work on this project. Here we thank them all.

Bibliography

[1] Теленин, Г. Ф., Тиняков, Г. П., Метод расчета пространственного обтекания тел с отошедшей ударной волной, *ДАН СССР*, 154, 5 (1964).

[2] Гилинский, С. М., Теленин, Г. Ф., Тиняков, Г. П., Метод расчета сверхзвукового обтекания затупленных тел с отошедшей ударной волной, *ИАН СССР, ОТН, Механика и Машиностроение*, 4 (1964).

[3] Гилинский, С. М., Теленин, Г. Ф., Сверхзвуковое обтекание тел различной формы с отошедшей ударной волной, *ИАН СССР, ОТН, Механика и Машиностроение*, 5 (1964).

[4] Гилинский, С. М., Макарова, Н. Е., Расчет сверхзвукового обтекания затупленных тел потоком воздуха с учетам равновесных физико-химических превращений, *ИАН СССР, МЖГ*, 1 (1966).

[5] Стулов, В. П., Теленин, Г. Ф., Неравновесное обтекание сферы сверхзвуковым потокой воздуха, *ИАН СССР, Механика*, 1 (1965).

[6] Van Dyke, M. D., The supersonic blunt-body problem —— Review and extension, *J. A. S.*, 25, 8 (1958).

[7] Белоцерковский, О. М., Симметритное обтекание затупленных тел сверхзвуковым потоком совершенного и реального газа, *Ж. ВММФ*, 2, 6 (1962).

[8] Vaglio-Laurin, R., Ferri, A., Theoretical investigation of flow field about blunt-nosed bodies in supersonic flight, *J. A. S.*, 25, 12 (1958).

[9] Белоцерковский, О. М., Расчет обтекания осесимметритных тел с отошедшей ударной волной (Расчетные формулы и таблицы полей течений), ВЦ АН СССР, М. (1961).

[10] Годунов, С. К., Забродин, А. В., Прокопов, Г. П., Разностная схема для двухмерных нестационарных задач газовой динамики и расчет обтекания с отошедшей ударной волной, *Ж. ВММФ*, 1, 6 (1961).

[11] Бабенко, К. И., Русанов, В. В., Разностные методы решения пространственных задач газовой динамики, Труды II, Всесоюз. Съезда по Теорет. и Прикл. Механ., М. (1965).

* [12] 陈炳木，平衡状态下空气的几种热力学函数的近似计算，力学，3 (1977).

[13] Moretti, A., A fast direct and accurated technique for blunt body problem, General Applied Science Labs Inc., TR 583 (1966).

[14] Тиняков, Г. П., Исследование трехмерного сверхзвукого обтекания эллипсоидов вращения, *ИАН СССР, Механика*, 6 (1965).

[15] Белоцерковский, О. М., Обтекание затупленных тел сверхзвуковым потоком газа (Теоретическое и экспериментальное исследования), ВЦ АН СССР, М. (1966).

[16] Теленин, Г. Ф., Тиняков, Г. П., Метод расчета пространственного обтекания тел с отошедшей осесимметричных тел с отошедшей ударной волной, ВЦ АН СССР, М. (1961).

* 12. Chen Bing-mu, The Approximate Calculation of a Few Kinds of Thermodynamic Function of Air Under Balanced State, Mechanics, 3 (1977)

DISTRIBUTION LIST

DISTRIBUTION DIRECT TO RECIPIENT

ORGANIZATION		MICROFICHE
A205	DMATC	1
A210	DMAAC	2
B344	DIA/RDS-3C	9
C043	USAMIIA	1
C509	BALLISTIC RES LABS	1
C510	AIR MOBILITY R&D LAB/FIO	1
C513	PICATINNY ARSENAL	1
C535	AVIATION SYS COMD	1
C591	FSTC	5
C619	MIA REDSTONE	1
D008	NISC	1
H300	USAICE (USAREUR)	1
P005	DOE	1
P050	CIA/CRB/ADD/SD	2
NAVORDSTA (50L)		1
NASA/NST-44		1
AFIT/LD		1
LLL/Code L-389		1
NSA/1213/TDL		2

ORGANIZATION		MICROFICHE
E053	AF/INAKA	1
E017	AF/RDXTR-W	1
E403	AFSC/INA	1
E404	AEDC	1
E408	AFWL	1
E410	ADTC	1
	FTD	
	CCN	1
	ASD/FTD/NIIS	3
	NIA/PHS	1
	NIIS	2